

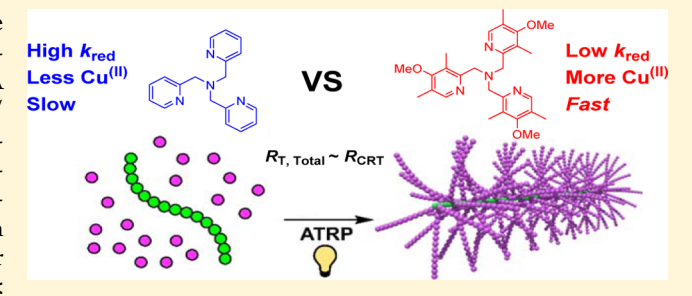
Understanding the Relationship between Catalytic Activity and Termination in photoATRP: Synthesis of Linear and Bottlebrush **Polyacrylates**

Michael R. Martinez, Julian Sobieski, Francesca Lorandi, Marco Fantin, Sajjad Dadashi-Silab, Guojun Xie, Mateusz Olszewski, Xiangcheng Pan, Thomas G. Ribelli, and Krzysztof Matyjaszewski Thomas G. Ribelli, and Krzysztof Matyjaszewski

Department of Chemistry, Center for Macromolecular Engineering, Carnegie Mellon University, 4400 Fifth Avenue, Pittsburgh, Pennsylvania 15213, United States

Supporting Information

ABSTRACT: Linear and bottlebrush polyacrylates were prepared by photomediated atom transfer radical polymerization (photoATRP) catalyzed by either CuBr₂/TPMA (tris(2-pyridylmethyl)amine) or the more active CuBr₂/ TPMA*³ (tris([(4-methoxy-2,5-dimethyl)-2-pyridyl] methyl)amine). The latter had a lower rate constant of photoreduction (k_{red}) but unexpectedly enabled faster polymerization. Kinetic simulations showed that the equilibrium concentration of a Br-CuII/L deactivator was larger for CuBr₂/TPMA*³, resulting in a faster reduction rate ($R_{\rm red} \propto$



 $k_{\rm red}[{\rm Br-Cu^{II}/L}])$ and higher radical concentration. At the same time, the low $[{\rm Cu^I/TPMA^{*3}}]$ counterweighed its high tendency to promote catalyzed radical termination (CRT), and the CRT rate was similar for the two catalytic systems. Kinetic simulations proved that (i) relative reaction rates cannot be predicted by the rate constant alone as exhibited by the relative amount of Cu and Cu^{II} species mediated by catalyst activity and termination selectivity and (ii) the polymerization steady state is reached faster with more active catalysts. With this understanding, polyacrylate bottlebrushes were synthesized at moderately high conversion by photoATRP.

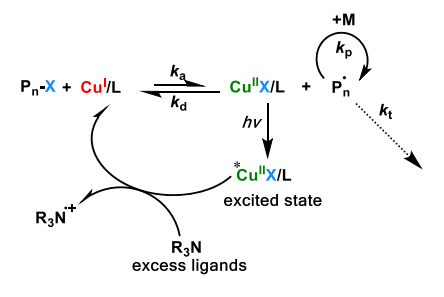
■ INTRODUCTION

Controlled radical polymerization techniques, such as reversible addition-fragmentation chain transfer (RAFT) polymerization, 1,2 nitroxide-mediated polymerization, 3-5 and atom transfer radical polymerization (ATRP),6-11 have allowed for the preparation of materials with controlled composition and architecture. ATRP is one of the most widely used techniques because of its simple experimental setup and compatibility with a wide range of commercially available monomers, solvents, and initiators. Traditional (normal) ATRP employed a large amount of catalysts with limited activity to control the chain growth. As catalytic performance of Cu-based complexes improved through the design of new ligands (L), the catalyst loading could be lowered to parts-per-million (ppm) concentrations under conditions with continuous regeneration of the active Cu^I/L complex. 12

Recent ATRP techniques with low catalyst loading rely on in situ (re)generation of Cu^I/L activators through the use of thermal radical initiators (ICAR ATRP), ^{13,14} reducing agents (ARGET ATRP), ^{13,15,16} heterogeneous zerovalent metals (SARA ATRP), ^{17–22} or external stimuli such as electric current/potential (eATRP), ^{23–27} light, ^{28–37} and ultrasound.^{38,39} Regeneration of Cu^I/L activators through light exposure (photoATRP) is especially attractive for its simple reaction setup, slight oxygen tolerance, mild conditions, and

spatial and temporal control over polymerization.^{37,40-44} PhotoATRP is based on a photoinduced reductive quenching mechanism between an electron-donor (a tertiary amine or excess ligands) and the excited X-Cu^{II}/L deactivator, resulting in Cu^I/L activator (re)generation and can allow for ppm loadings of the catalyst (Scheme 1). 32,33,44 Recent reports have employed transition metal-based-35,45 or organo-photocatalysts 45-50 to conduct ATRP. Similar works have used triplet energy transfer (energy/electron exchange) of photocatalysts

Scheme 1. Mechanism of PhotoATRP



Received: November 13, 2019 Revised: December 12, 2019 Published: December 31, 2019

to generate radicals in photoinduced electron/energy transfer RAFT polymerization (PET-RAFT). $^{51-54}$

The regeneration of active species through external stimuli presents a unique challenge for highly active catalytic complexes. The rate of polymerization (R_p) in systems with activator regeneration and strictly conventional biradical termination is proportional to the square root of the ratio of the rate of reduction to rate constant of termination, that is $(R_{\rm red}/k_{\rm t})^{1/2}$, according to eq 1, where RA is the reducing agent. Thus, polymerization rate is enhanced by faster reduction of the X-Cu^{II}/L deactivator and a low rate constant of termination. ⁵⁵

$$R_{p} = k_{p}[M][R^{\bullet}] = k_{p}[M] \sqrt{\frac{R_{red}}{k_{t}}} = k_{p}[M]$$

$$\sqrt{\frac{k_{red}[RA][X - Cu^{II}L]}{k_{t}}}$$
(1)

High ATRP catalytic activity correlates to more negative standard reduction potentials thus requiring the use of powerful reductants to achieve an efficient regeneration of the activator Cu^I/L complex.⁵⁵ In the case of photoATRP, a mild alkylamine reducing agent induces the reductive quenching of the excited Br-CuII/L*. The interplay between rate of polymerization and redox properties of ATRP catalysts was highlighted in the recent work addressing temporal control in ATRP in the presence of zerovalent metals.⁵⁶ When ATRP was conducted with Ag⁰ as a reducing agent, the overall rate of the reaction decreased with increasing catalyst activity (i.e. larger ATRP equilibrium constant, K_{ATRP}). Conversely, SARA ATRP using Cu0 under similar conditions followed the expected increase in the rate of polymerization with catalytic activity. Thus, it is apparent that the relationship between X-Cu^{II}/L reduction, catalytic activity, and termination needs to be considered in activator (re)generation systems.

Termination in ATRP proceeds via conventional biradical termination (RT) and/or catalyzed radical termination (CRT). The latter is the main mode of termination for acrylate radicals in the presence of Cu catalysts with a high ATRP activity (i.e. high $K_{\rm ATRP}$). CRT proceeds via reversible coordination of radicals to Cu^I/L to form an organometallic P_n –Cu^{II}/L complex, as shown in Scheme 2. $^{5S,58-60}$ P_n –Cu^{II}/L can then react with a second radical to

Scheme 2. Formation of Paramagnetic Organometallic Species in ATRP, Following a Typical Organometallic-Mediated Radical Polymerization Equilibrium, with Subsequent CRT Step Leading to Terminated Chains and Regeneration of Cu¹/L Species

$$\frac{\text{Cu}^{1}/\text{L}}{\text{R}^{\bullet}} + P_{\text{n}}^{\bullet} \xrightarrow{\text{KoMRP}} P_{\text{n}} - \text{Cu}^{1}/\text{L} \xrightarrow{\text{R}^{\bullet}} \text{Cu}^{1}/\text{L} + \text{termination products}$$

$$\frac{\text{R}^{\bullet}}{k_{\text{CRT}}^{\bullet}}$$

form dead chains with concurrent regeneration of Cu^I/L . In addition, it was recently proposed that P_n-Cu^{II}/L can react with protic impurities or hydrogen atom donors to form dead chains and an inactive Cu^{II} species, according to a reductive radical termination mechanism.

CRT is generally considered to be an unwanted termination side-reaction because it contributes to decreased polymerization livingness. However, CRT can be used as a tool to

tailor ATRP products. ⁶³ Indeed, CRT could be exploited to diminish coupling between large polyfunctional polyacrylates thus mitigating gelation and allowing for faster reaction times. Unlike biradical combination, termination by CRT gives chains of the same molecular weight as the original terminating chains and prevents chains from combining. Large 372-arm poly(*n*-butyl acrylate) (PBA) brushes were prepared at over 90% conversion by grafting-from ATRP, while maintaining very low degree of coupling by using CRT-promoting conditions. ⁶³

This work investigates the role of ATRP catalysts activity in determining polymerization rates and the extent of different radical termination pathways in photoATRP. The investigation was aimed to identify CRT-promoting conditions under UV light irradiation for the preparation of molecular bottlebrushes by photoATRP. Two catalysts were employed: Cu/tris(2pyridylmethyl)amine (Cu/TPMA) and the highly active Cu/ tris([(4-methoxy-2,5-dimethyl)-2-pyridyl] methyl)amine (Cu/ TPMA*3). These two catalysts were chosen because of their similarity in structure but large difference in activity with Cu/ TPMA*3 being 500 times more active than Cu/TPMA.64,65 Moreover, the two catalysts exhibited different rate constants of photoreduction, which depends on both redox and optical properties, and different abilities to promote CRT. With the aid of kinetic simulations, we defined how polymerization kinetics and controls are linked to the ATRP equilibrium constant, photoreduction rate, termination selectivity, and termination rates by CRT and RT. Our findings were then applied to synthesize polyacrylate brushes at moderately high conversion by photoATRP via the grafting-from approach.

■ RESULTS AND DISCUSSION

Polymerization of *n*-Butyl Acrylate by PhotoATRP. The photopolymerization of *n*-butyl acrylate (BA) with Cu/ TPMA or Cu/TPMA*3 and a small molecule initiator (ethyl α -bromoisobutyrate, EBiB) was selected as a model system to investigate the role of catalyst activity and concentration in photoATRP. A 16 vol % dimethylformamide (DMF)/64 vol % anisole cosolvent system was utilized because of the large differences in solubility between nonpolar PBA and polar Cu/ L complexes. Anisole helped in solubilizing nonpolar PBA, while the small addition of DMF ensured that the Cu/L catalyst did not crash out of the mostly nonpolar reaction medium. The results of model polymerizations are summarized in Table 1 and Figure 1. Reactions are listed in Table 1 in the format L-X, where L is the ligand (T refers to TPMA, T*3 to TPMA*3) and X is catalyst loading expressed in ppm relative to monomer concentration.

PhotoATRP of BA with EBiB as a small molecule initiator showed a pronounced increase in the rate of polymerization by increasing the catalytic activity and diminishing the catalyst concentration. The apparent rate of polymerization ($k_{\rm p}^{\rm app}$) for the polymerization conducted with 190 ppm Cu/TPMA was 0.064 h⁻¹, while the polymerization conducted under similar conditions but with 190 ppm of the more active catalyst Cu/TPMA*³ was 2.5 times faster with a $k_{\rm p}^{\rm app}$ of 0.156 h⁻¹ and comparable control (Table 1). All polymerization reactions using the Cu/TPMA*³ catalyst proceeded with comparable control and were 2–3 times faster than the corresponding polymerization using Cu/TPMA. However, Br–Cu^{II}/TPMA*³ has a much more negative reduction potential than Br–Cu^{II}/TPMA, and thus, it should be reduced more slowly. According to eq 1, the slower reduction of [Br–Cu^{II}/TPMA*³] was

Table 1. Reaction Conditions for the PhotoATRP of BAa

reaction entry	$[BA]:[EBiB]:[CuBr_2]:[L]$	ligand (L)	[CuBr ₂] (ppm)	$k_{\rm p}^{\rm app}^{b}$ (h ⁻¹)	time (h)	monomer conversion	$M_{ m n,app}^{c}$	$M_{ m n,th}$	\mathcal{D}^{c}
T-760	160:1:0.12:0.24	TPMA	760	0.012	72	0.63	13.5	12.7	1.11
T-190	160:1:0.03:0.06	TPMA	190	0.064	24	0.76	15.4	14.5	1.15
T-32	160:1:0.005:0.01	TPMA	32	0.077	13	0.64	11.9	12.9	1.41
T^{*3} -760	160:1:0.12:0.24	TPMA*3	760	0.075	27	0.87	15.5	17.6	1.14
T^{*3} -190	160:1:0.03:0.06	TPMA*3	190	0.156	6	0.59	12.6	11.9	1.14
$T^{*3}-32$	160:1:0.005:0.01	TPMA*3	32	0.193	6	0.67	13.8	13.6	1.24

"Solvent content: 16 vol % DMF and 64 vol % anisole. Temperature: room temperature. Wavelength of irradiation: 360 nm, 4.9 mW/cm². "Slope of the first order kinetic plots is shown in Figure 1a. "Molecular weight and dispersity from GPC calibrated against polystyrene standards in THF at a temperature of 30 °C (see Figure S1 in the Supporting Information).

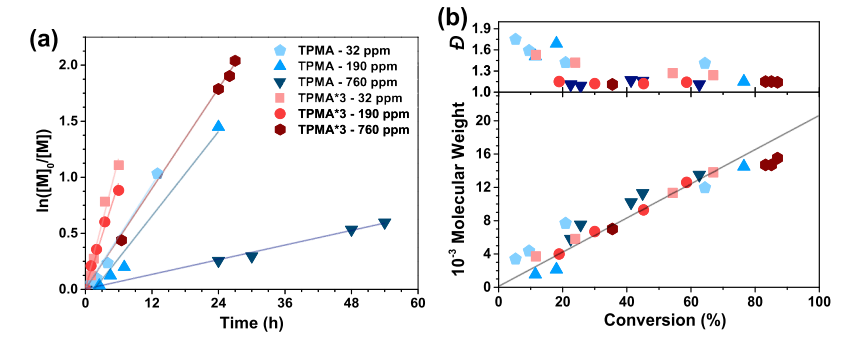


Figure 1. (a) First order kinetic plots and (b) molecular weight and dispersity evolution in the polymerization of BA with 760, 190, or 32 ppm of the Cu/TPMA or Cu/TPMA* 3 catalyst. Irradiation at 360 nm and 4.9 mW/cm 2 at room temperature with 16 vol % DMF and 64 vol % anisole. [BA]:[EBiB]:[CuBr₂]:[L] = 160:1:x:2x, x = 0.12, 0.03, or 0.005.

expected to result in slower polymerization catalyzed by Cu/TPMA*³ compared to Cu/TPMA under similar conditions.

Variations in the catalyst concentration affected both the rate and control on polymerization. The rate of polymerization with Cu/TPMA*³ was 6 times higher when catalyst loading ([Cu^{II}Br₂]₀, with [Cu^{II}Br₂]₀:[L]₀ = 1:2) was decreased from 760 to 32 ppm (Table 1) although the reduction rate should increase with [Br–Cu^{II}/L]¹¹² (eq 1). This could be attributed to a lower optical density under more dilute conditions, promoting faster photoreduction. Moreover, a lower catalyst loading means a lower equilibrium concentration of Cu¹/L, and therefore, a decreased extent of termination by CRT, which could result in faster polymerization in the case of a significant amount of terminated chains. 57

Control over polymerization decreased at low $[Cu^{II}Br_2]_0$. Both Cu/TPMA and $Cu/TPMA^{*3}$ catalytic systems showed an increase in the dispersity of the prepared homopolymers by decreasing $[Cu^{II}Br_2]_0$ from 760 to 32 ppm. The TPMA-based system exhibited a larger increase in polymer dispersity, from $\mathcal{D}=1.11$ to 1.41. The effect of catalyst loading on polymerization control was exploited to tune the dispersity of linear polyacrylates in photoATRP. ^{66,67}

Photoreduction of Copper Complexes. In order to better understand the difference in polymerization rate between the Cu/TPMA and Cu/TPMA*3 systems, photoreduction of both Br–Cu^{II}/L catalysts at varying concentrations was monitored via UV/vis spectroscopy in the absence of EBiB and BA (Section S3, Supporting Information). It should be noted that different reduction rate constants were obtained for the same catalyst at different concentrations (Table 2). In particular, the reduction rate constant increased with decreasing [Br–Cu^{II}/TPMA]₀. This could be attributed to increased absorbance or reduced transmittance of the solution at higher catalyst loading. Therefore, the rate

Table 2. Observed Rate Constants of Br-Cu^{II}/L Reduction $(k_{\text{red,obs}})$ and Rate Constants of Apparent CRT $(k_{\text{CRT,app}})$ for L = TPMA and TPMA*³.

ligand	$[Br-Cu^{II}/L]_o$ (ppm)	$k_{\rm red,obs} \ (10^6 \ {\rm s}^{-1})^a$	$k_{\rm CRT,app} \ (10^{-4} \ {\rm s}^{-1})^{L}$
TPMA	760	4.2 ± 0.2	2.4 ± 1.3
	190	54 ± 3	0.91 ± 0.12
	32	78 ± 8	1.1 ± 0.3
TPMA*3	190	20 ± 0.7	44 ± 20

^aConditions: irradiation at 360 nm and 4.9 mW/cm² at room temperature in 16 vol % DMF and 64 vol % anisole. ^bObtained via Predici parameter estimation.

constants of reduction measured through this technique are formally observed as apparent reduction rate constants, $k_{\rm red,obs}$.

At identical loading concentrations, Br-Cu^{II}/TPMA was reduced faster than Br-Cu^{II}/TPMA*³ (Figure 2, Table 2), as expected on the basis of the redox properties of the complexes. This suggests that the Cu/TPMA system has a lower concentration of the deactivator under polymerization

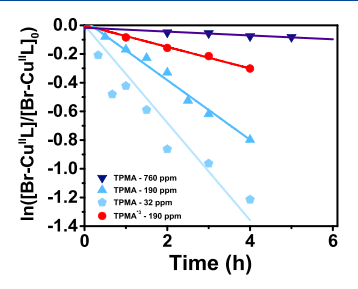


Figure 2. Photoreduction of Br–Cu II /L complexes of varying concentrations upon irradiation by UV light at 360 nm and 4.9 mW/cm 2 at room temperature with 16 vol % DMF and 64 vol % anisole.

Table 3. Kinetic Model for the photoATRP of Butyl Acrylate Mediated by Cu/L and Initiated by EBiB

		value						
reaction	constants	L = TPMA	$L = TPMA*^3$	refs				
Catalyst Regeneration								
$Br-Cu^{II}/L \rightarrow Cu^{I}/L(+Br^{-})$	$k_{ m red,obs}~({ m s}^{-1})$	Table 2						
ATRP								
$R-Br + Cu^{I}/L \rightleftharpoons R^{\bullet} + Br-Cu^{II}/L$	$K_{\text{ATRP,RX}}/k_{\text{a,RX}} (M^{-1} \text{ s}^{-1})/k_{\text{d,RX}} (M^{-1} \text{ s}^{-1})$	$1.0 \times 10^{-6}/15/1.5 \times 10^{7}$	$8.0 \times 10^{-4}/1.6 \times 10^{4}/1.5 \times 10^{7}$	69 ^a				
$P_n - Br + Cu^I/L \rightleftharpoons P_n^{\bullet} + Br - Cu^{II}/L$	$K_{\text{ATRP}}/k_{\text{a}} (M^{-1} \text{ s}^{-1})/k_{\text{d}} (M^{-1} \text{ s}^{-1})$	$2.6 \times 10^{-8} / 0.80 / 3.0 \times 10^{7}$	$1.3 \times 10^{-5}/4.0 \times 10^{2}/3 \times 10^{7}$	58 ^a				
Apparent CRT								
$P_n^{\bullet} + Cu^I/L \rightarrow Cu^I/L + dead chains$	$k_{\rm CRT,app}~({ m M}^{-1}~{ m s}^{-1})$	$(1.5 \pm 0.7) \times 10^{4b}$	$(4.4 \pm 2.0) \times 10^5$	а				
Addition and Propagation								
$R^{\bullet} + M \rightarrow P_1^{\bullet}$	$k_{\rm add,RX}~(\mathrm{M}^{-1}~\mathrm{s}^{-1})$	1.4×10^{3}	70					
$P_n^{\bullet} + M \rightarrow P_{n+1}^{\bullet}$	$k_{\rm p} \ ({ m M}^{-1} \ { m s}^{-1})$	2.0×10^4	71					
Conventional Radical Termination (RT)								
$P_n^{\bullet} + P_m^{\bullet} \rightarrow P_n - P_m$	$2 \times k_{\rm t} ({ m M}^{-1} { m s}^{-1})$	3×10^{7}	72					
$P_n^{\bullet} + R \rightarrow P_n - R$	$2 \times k_{\text{t,mix}} (\mathrm{M}^{-1} \mathrm{s}^{-1})$	1×10^{8}	55					
$R^{\bullet} + R^{\bullet} \rightarrow R - R$	$2 \times k_{\rm t,R} \ ({ m M}^{-1} \ { m s}^{-1})$	2×10^9	55					
$^{a}k_{d,RX}$, k_{d} , and $k_{CRT,app}$ were obtained in this work. b averaged from Table 2.								

conditions than an analogous system with Cu/TPMA*³. Simulations indicate that the difference in [Br–Cu^{II}/L] must outweigh the reduction rate constant for establishing a higher rate of reduction for the catalyst with lower $k_{\rm red,obs}$. Overall, higher resultant $R_{\rm red}$ drives a higher rate of polymerization, regardless if the system has a lower $k_{\rm red,obs}$.

Simulation of PhotoATRP Mechanism. The reaction rates, catalyst species, and termination products for the photoATRPs of BA with EBiB as an initiator and catalyzed by Cu/TPMA and Cu/TPMA*3 were concurrently investigated through kinetic simulations to gain further insight into the process and relative termination pathways and reduction rates for each system (Figure 4). Simulations were performed using the software Predici (version 6.3.1; CiT, Computing in Technology). 68 The experimental data for the polymerization of BA with 190 ppm of Br-CuII/L (Table 1) were fitted to the model presented in Table 3, which included the following reactions: (i) reduction of Br-Cu^{II}/L ($k_{red,obs}$), (ii) ATRP equilibrium (K_{ATRP}) with activation and deactivation rate constants of dormant chains (k_a, k_d) and alkyl halide initiators $(k_{a,RX}, k_{d,RX})$, (iii) radical propagation (k_p) , (iv) addition of the initiating ethyl α -isobutyrate radical to BA ($k_{\text{add,RX}}$), and (v) conventional bimolecular radical termination (RT) between polymers and small-molecule species $(k_{tc}, k_{t,mix}, k_{t,R})$. Additionally, to account for the CRT reaction without disposing of kinetic information on the formation and stability of the P_n-Cu^{II}/L intermediate in the analyzed systems, an apparent CRT reaction was defined as follows: $Cu^I/L + P_n^{\bullet} \rightarrow Cu^I/L +$ terminated chains with rate constant $k_{\text{CRT,app}}$. The latter can be related to the rate constants of association/dissociation of P_n Cu^{II}/L and the rate constant of CRT as described in Section S4.2 of Supporting Information. Finally, the effect of backbiting on overall kinetics was small and thus not considered (Section S4.3 of Supporting Information).

Most of the thermodynamic and kinetic parameters required for simulations were retrieved from the literature or independently measured as described in Sections S3 and S4 of Supporting Information. Two remaining unknown parameters, $k_{\text{CRT,app}}$ and k_{d} , were adjusted by fitting the simulated curves to the experimental kinetic and dispersity data, respectively. $k_{\text{CRT,app}}$ and k_{d} are treated as orthogonal parameters because $k_{\text{CRT,app}}$ influences the polymerization kinetics (Section S4.3), while k_{d} affects polymer dispersity as

the deactivator concentration is the dominant term on the polymerization control (Section S4.1). Good agreement between simulated and experimental data (Figure 3) confirmed the validity of the model as shown in Table 3.

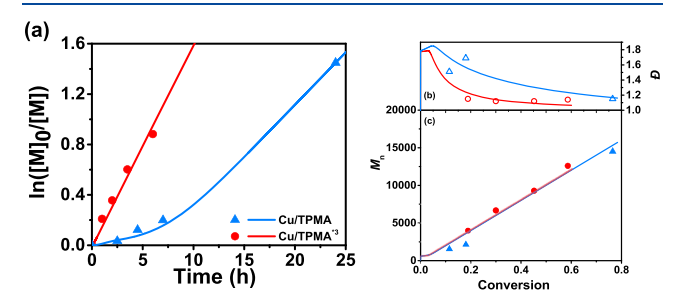


Figure 3. (a) First order kinetic plots; evolution of (b) dispersity and (c) molecular weight vs conversion for the photoATRP of BA initiated by EBiB and catalyzed by Cu/TPMA (blue) or Cu/TPMA*³ (red). Experimental data are represented by discrete points and the simulated outputs by lines. Conditions for Cu/TPMA and Cu/TPMA*³ correspond to T-190 and T*³-190 as shown in Table 1.

Kinetic simulations showed that Br-Cu^{II}/TPMA was reduced faster than Br-Cu^{II}/TPMA*³ at the beginning of polymerization (Figure 4c-e) as expected by $k_{\rm red,obs}$ of Br-Cu^{II}/TPMA being 2.7 times higher than $k_{\rm red,obs}$ for Br-Cu^{II}/TPMA*³ (Table 2). However, Cu/TPMA*³ showed a ~2.3 times higher reduction rate ($R_{\rm red} \propto k_{\rm red}[{\rm Br-Cu^{II}}/{\rm L}]$) at the catalyst steady state (Figure 4e) as it was accompanied by ~40 times higher [Br-Cu^{II}/TPMA*³] relative to [Br-Cu^{II}/TPMA] when both systems reached the steady state (i.e. the rate of reduction equaled the total rate of termination, $R_{\rm red} = R_{\rm T,TOTAL}$). This difference in the deactivator fraction also improved polymerization control, as experimentally observed. The fraction of the catalyst in the form of Br-Cu^{II}/L was significantly smaller in the case of Cu/TPMA throughout polymerization (Figure 4a), which ultimately hampered its rate of deactivation and catalyst regeneration (Figure 4e).

The simulated $R_{\rm p}$, $R_{\rm RT}$, $R_{\rm a}$, and $R_{\rm d}$ appeared to be discontinuous before the steady state was achieved (Figure 4c,d). Simulations attributed this fluctuation in reaction rates to differences between the rate constants of propagation, termination, activation, and deactivation for the tertiary α -

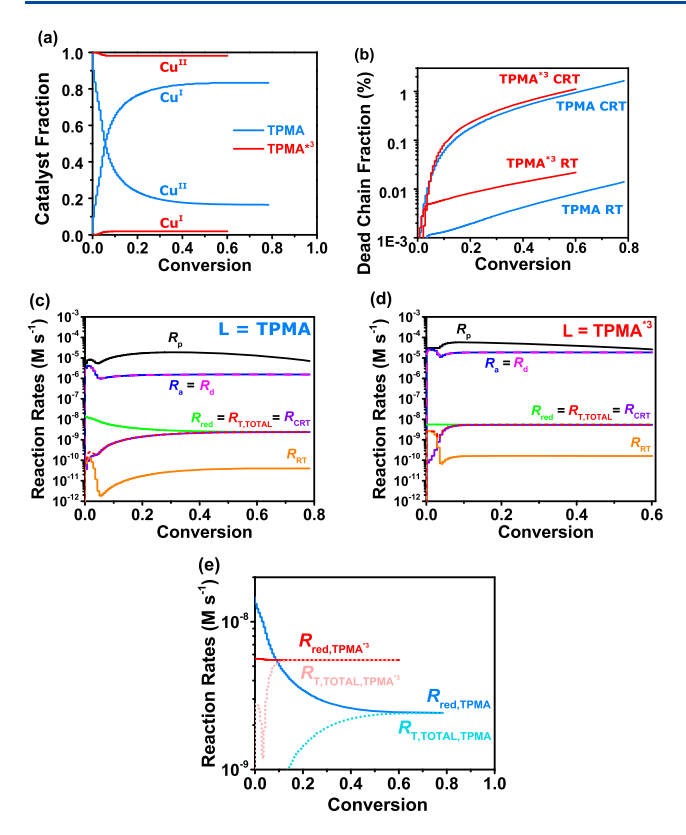


Figure 4. (a) Fraction of catalyst species, (b) total dead chain fraction by termination mechanism, (c,d) variation of reaction rates over time, and (e) evolution of reduction rate and total termination rate (i.e. sum of CRT and RT rates) with conversion as obtained from simulation of photoATRP of BA initiated by EBiB with Cu/TPMA and Cu/TPMA* 3 catalytic systems. Conditions: $[Cu^{II}Br_2]_0 = 190$ ppm relative to BA (2.7 × 10⁻⁴ M). Simulation time: 25 h for L = TPMA and 6 h for L = TPMA* 3 .

bromoisobutyrate initiator and the secondary acrylic BA chain end (Section S4.6).⁷³ The high activity (high K_{ATRP}) of EBiB and initial reduction of Br-Cu^{II}/L to Cu^I/L led to the first increase in R_a , R_d , R_p , and $R_{\rm RT}$ at this stage. Note that $R_a > R_{\rm red}$ at all stages for both catalysts, suggesting that every reduction event indirectly generates a radical. Then, R_p , R_a , and R_d decreased as chain ends transitioned from tertiary to secondary dormant species with incorporation of BA. During this process, Cu^I/L was still below the necessary concentration needed to establish a steady state ($R_{\text{red}} = R_{\text{T,TOTAL}}$). The accumulation of Cu^I/L caused R_a and R_d to increase slightly until this steady state was established. This fluctuation in reaction rates at the beginning of photoATRP would not be observed if methyl 2bromopropionate was used as initiator because K_{ATRP} of the initiator matches the dormant acrylic polymer chain end (Figure S10b).

It is worth noting that $R_{\rm red}$ decreased rapidly for the less active Cu/TPMA until the system reached its steady state at $\sim 60\%$ monomer conversion. Conversely, $R_{\rm red}$ remained approximately constant for the polymerization catalyzed by Cu/TPMA*³ in which the steady state was reached more quickly at $\sim 12\%$ monomer conversion. These observations demonstrate that $R_{\rm red}$ and consequently the polymerization rate cannot be predicted from $k_{\rm red,obs}$ because the distribution of Cu^I and Cu^{II} species strongly affects the kinetics. The catalyst fractions are mainly dictated by the ATRP activity of the catalyst; however, termination reactions need to be

considered as they can affect the establishment of the steady state and thus R_n at the steady state.

Termination rates and products were investigated by Predici simulations. The simulated total fraction of terminated chains in both polymerizations was \sim 1% at 60% monomer conversion (Figure 4b), indicating that both systems were highly living. The contribution of RT relative to CRT was higher in the case of Cu/TPMA*3 (Figure 4c,d) because of the overall higher radical concentration. However, the absolute contribution of CRT was similar for the two catalysts and significantly dominated RT with $R_{\rm CRT,app} > R_{\rm RT}$. Cu/TPMA*3 had ~30 times higher $k_{\rm CRT,app}$ compared to Cu/TPMA in agreement to the general observation that more active ATRP catalysts result in lower selectivity, that is, higher tendency to promote side reactions such as the formation of P_n -Cu^{II}/L and CRT.⁵⁸ The higher $k_{\mathrm{CRT,app}}$ together with the larger radical concentration resulted in slightly faster apparent CRT when using the more active catalyst despite [Cu¹/TPMA*³] being ~40 times lower than [Cu^I/TPMA] at the catalyst steady state. In summary, both catalysts reached similar $R_{\rm CRT,app}$ with that of Cu/TPMA*³ slightly higher than that of Cu/TPMA for different tendencies. Cu/TPMA generates a high fraction of Cu^I/ TPMA, while Cu/TPMA*3 has lower selectivity toward ATRP as a byproduct of its higher activity. This observation highlights the importance of moving toward more active and more selective ATRP catalysts which can both improve catalytic activity in ATRP and suppress side reactions which diminish chain end functionality.

The total rate of termination $(R_{T,TOTAL} = R_{RT} + R_{CRT})$ was slightly higher for Cu/TPMA*3 than for Cu/TPMA. The former reached ~1% dead chains in 6 h, while the latter did so in 25 h (Figures 4b and S11). At the catalyst steady state with $R_{\rm red} = R_{\rm T,TOTAL}$, both $R_{\rm T,TOTAL}$ and $R_{\rm red}$ were ~ 2.3 times higher for Cu/TPMA*3, resulting in higher R_p . This is in good agreement with experimental data that showed 2.4 times higher $k_{\rm p}^{\rm app}$ for Cu/TPMA*3 than that for Cu/TPMA (Table 1, Entries T-190 and T* 3 -190). The increase in R_{T,TOTAL} for Cu/ TPMA*3 was significant enough to increase catalyst regeneration but not high enough to alter kinetics via excessive chain death. It is evident that catalyst regeneration and termination are codependent in tuning R_p of these regenerative ATRP systems, where slightly increased termination can supply a higher steady state of the deactivator. Figure 4e illustrates a very interesting behavior: Br-Cu^{II}/TPMA is initially reduced faster, but as its concentration rapidly decreases, the overall rate of reduction becomes smaller for Br-Cu^{II}/TPMA*³. This is also reflected in twice slower termination in the former system. The steady state between reduction and termination is reached also much slower only at ca. 50% monomer conversion for Cu/TPMA.

In summary, kinetic simulations of photoATRP highlighted that (i) reaction rates depend on both rate constants and concentrations of reagents, which are determined by the reactivity of the species and their involvement in side reactions (i.e. selectivity); (ii) the more active catalyst Cu/TPMA*³ exhibited a lower rate constant of reduction but enabled higher $R_{\rm red}$ because of its significantly higher ratio of [Br–Cu^{II}/L]/[Cu^I/L] relative to Cu/TPMA, which resulted in higher $R_{\rm p}$; (iii) both systems showed predominant termination through CRT, where CRT was driven by the high fraction of Cu^I/L for Cu/TPMA and by the higher $k_{\rm CRT,\ app}$ for the more active and thus less selective Cu/TPMA*³; and (iv) despite eq 1 being valid for systems with termination by conventional RT, the

Table 4. Synthesis of PBA Molecular Bottlebrushes by photoATRP^a

reaction entry	$[BA]:[BiBEM]:[CuBr_2]:[L]$	ligand (L)	[CuBr ₂] (ppm)	$k_{\mathrm{p}}^{\mathrm{app}\boldsymbol{b}}$ (h ⁻¹)	time (h)	monomer conversion	grafting density
B-T-190	160:1:0.03:0.06	TPMA	190	0.038	30	0.67	0.78
B-T-32	160:1:0.005:0.01	TPMA	32	0.087	10	0.56	0.46
B-T*3-190	160:1:0.03:0.06	TPMA*3	190	0.073	8	0.44	0.77
$B-T*^3-32$	160:1:0.005:0.01	TPMA*3	32	0.276	3	0.57	0.66

^aSolvent content: 16 vol % DMF and 64 vol % anisole. Temperature: room temperature. Macroinitiator: PBiBEM backbone of DP 372. Wavelength of irradiation: 360 nm, 4.9 mW/cm². ^bSlope of the first order kinetic plot shown in Figure 5a.

polymerization rate was primarily dictated by $R_{\rm red}$ even when termination occurred predominately through CRT.

Synthesis of PBA Molecular Bottlebrushes. Even a small amount of biradical termination via combination has disastrous effects on the polymerization of large, multifunctional, bottlebrush polymers in which macroscopic gelation could occur. Grafting-from ATRP of BA from a poly(2-bromoisobutyryloxyethyl methacrylate) (PBiBEM) polymer with a degree of polymerization (DP) equal to 372 was used to investigate the effect of the termination pathways of Cu/TPMA and Cu/TPMA*³ catalysts in photoATRP. The relative weight fraction of "coupling" determined by gel permeation chromatography (GPC) (Figure S13 in Supporting Information) gave insight into the amount of intermolecular termination by biradical combination in polymerization.

The catalyst nature is also expected to affect the grafting density, which in turn influences the conformation of bottlebrushes in melt and solution and dictates their material properties. The grafting densities of the final products were quantified by side chain cleavage in which PBA side chains were cleaved via solvolysis and analyzed via GPC to obtain the molecular weights (Section S5.1 in Supporting Information). Table 4 summarizes the reaction conditions used to synthesize molecular bottlebrushes. Each entry is listed in format B–L–X, where B denotes a brush prepared via grafting-from polymerization with ligand L (T still refers to TPMA, T*3 to TPMA*3) and X is the catalyst loading expressed in ppm relative to monomer concentration.

As in model experiments with a small molecule initiator (Table 1), $k_{\rm p}^{\rm app}$ substantially increased with decreasing initial catalyst concentration for both catalytic systems. Grafting-from photoATRP in the presence of 190 ppm of Cu/TPMA*³ had a $k_{\rm p}^{\rm app}$ of 0.073, while a considerably higher $k_{\rm p}^{\rm app}$ of 0.276 was obtained when employing only 32 ppm of Cu/TPMA*³. Both catalyst loadings effectively suppressed biradical combination, as B–T*³-32 had 12% of chains terminated by radical coupling at 32% monomer conversion while B–T*³-190 had 11% at 36% conversion (Figure 5b). The evolution of the weight fraction of the coupled brushes with conversion was similar for all catalysts and concentrations, which could be attributed to the overall low fraction of dead chains and $R_{\rm CRT} \approx R_{\rm T,TOTAL}$ for both Cu/TPMA and Cu/TPMA*³ systems.

A comparison between B–T*³-190 and B–T-190 highlights the relationship between catalytic activity and corresponding radical termination pathways in photoATRP. Both systems showed minimal increase in the fraction of coupled brushes with conversion however slightly less radical coupling occurred in B–T-190. This trend agrees with simulations showing a smaller fraction of RT terminated chains in model polymerization (Figure 4b) and an overall high livingness of both systems. Moreover, the photoATRP catalyzed by Cu/TPMA was considerably slower than with Cu/TPMA*³ in agreement with simulations.

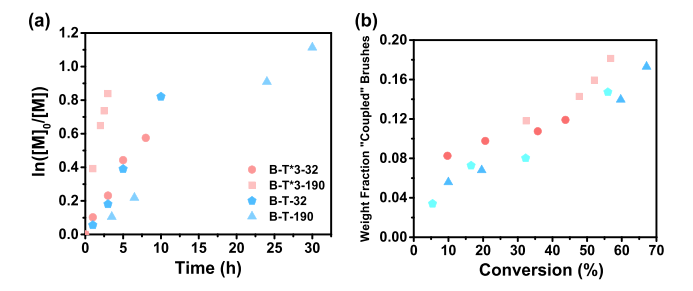


Figure 5. (a) First order kinetic plots for the polymerization of PBA molecular bottlebrushes and (b) Evolution of intermolecular termination by radical coupling with conversion. Conditions as in Table 4. Irradiation: $\lambda = 360$ nm, energy density = 4.9 mW/cm² with 16 vol % DMF and 64 vol % anisole.

The control over polymerization using both catalysts was good with grafting densities of 77 and 78% for B-T-190 and B-T*3-190, respectively (Table 4). A grafting density below 100% was expected as initiation efficiency on the surface of a polymer brush is lower than that of analogous small molecule initiators because of significant steric hindrance between neighboring side chains. Moreover, polymer brushes synthesized under low-ppm catalyst loadings had lower grafting densities than the reactions conducted with relatively higher loadings because of the lower concentration of Br-CuII/L deactivators at low-ppm loadings.⁷⁷ When copper concentration is low, there is a slower initiation and slower deactivation, and longer chains grow with a broader distribution of molecular weights. This was also observed in the model polymerization with EBiB as the initiator (Table 1) in which PBA dispersity increased with decreasing [CuBr₂]₀, especially for the Cu/TPMA system. For a molecular bottlebrush, inefficient deactivation leads to a smaller number of growing side chains. If the amount of deactivators is low, relatively long side chains grow and sterically shield neighboring initiating sites from the catalyst, causing the grafting density to decrease.⁶⁷ Therefore, the discrepancy in initiation efficiency (i.e. grafting density for bottlebrushes) between polymerization with a small molecule initiator and grafting-from polymerizations and between different catalyst loadings could be attributed to slow deactivation. In particular, in B-T*3-32 the fraction of the Br-Cu^{II}/L deactivator was higher because of the higher ATRP activity of Cu/TPMA*3 compared to Cu/TPMA, resulting in improved initiation efficiency, that is, higher grafting density than in B-T-32 (Table 4).

CONCLUSIONS

Kinetic analysis of Cu-mediated photoATRP of BA was conducted using a combination of experiments and simulations. The differences in polymerization rates obtained by using catalysts with different ATRP activity could be

rationalized by differences in catalyst activity mediating their respective catalyst fractions. In photoATRP catalyzed by Cu/TPMA, the fraction of the Br–Cu^{II}/L deactivator was significantly lower than that when using the more active Cu/TPMA*³. The low [Br–Cu^{II}/TPMA] at the catalyst steady state led to a lower rate of reduction. Conversely, in photoATRP catalyzed by Cu/TPMA*³, a high fraction of the deactivator was present, leading to a higher rate of reduction despite $k_{\rm red,obs}$ for Br–Cu^{II}/TPMA being higher than $k_{\rm red,obs}$ for Br–Cu^{II}/TPMA*³. Overall, the rate of propagation was found to depend on the rate of reduction, which is a product of both deactivator concentration and reduction rate constant.

For both catalytic systems, CRT was the predominant mode of chain termination, not RT. This resulted from the high fraction of $\mathrm{Cu^I}/\mathrm{L}$ for the system catalyzed by $\mathrm{Cu}/\mathrm{TPMA}$ and from the higher efficiency in promoting CRT for $\mathrm{Cu}/\mathrm{TPMA}^{*3}$. By using $\mathrm{Cu}/\mathrm{TPMA}^{*3}$, the catalyst steady state was reached more quickly and at lower monomer conversion compared to the $\mathrm{Cu}/\mathrm{TPMA}$ system. Therefore, despite that more active ATRP catalysts are typically more difficult to reduce and have lower selectivity toward the ATRP equilibrium, their high K_{ATRP} results in high $\mathrm{[Br-Cu^{II}/L]/[Cu^{I}/L]}$, which enables faster overall photoreduction and improved control.

PhotoATRP with a small molecule initiator and Cu/ TPMA*3 as a catalyst yielded polymers with lower dispersity than analogous reactions conducted with Cu/TPMA, in agreement with simulations, as the presence of high [Br-Cu^{II}/TPMA*³] enhanced the control. The predominant termination by CRT over RT for both Cu/TPMA and Cu/ TPMA*3 systems could be exploited to synthesize well-defined polymer brushes with little coupling as bimolecular termination was significantly lower than CRT. Decreasing the catalyst loading to 32 ppm resulted in faster, more uncontrolled polymerizations for both bottlebrushes and linear polymers. Linear PBA showed a pronounced increase in dispersity from D = 1.11 with 760 ppm of Cu/TPMA to D =1.41 with 32 ppm of Cu/TPMA. A much smaller increase in dispersity was observed with the more active Cu/TPMA*3 under similar conditions (from D = 1.14 to 1.24) because of the relatively larger fraction of the Br-Cu^{II}/TPMA*³ deactivator. Bottlebrushes prepared using low ppm photo-ATRP suffered from inefficient deactivation of growing side chains, which resulted in grafting densities of 46 and 66% when using 32 ppm of Cu/TPMA and Cu/TPMA*3, respectively. Higher catalyst loading improved the efficiency of deactivation and at the same time promoted CRT, allowing for the preparation of brushes with grafting densities of >75% and minimal coupling. Only a small fraction of bottlebrush side chains were terminated by radical coupling under all polymerization conditions.

ASSOCIATED CONTENT

S Supporting Information

The Supporting Information is available free of charge at https://pubs.acs.org/doi/10.1021/acs.macromol.9b02397.

Experimental procedures, GPC traces, kinetic plots, detailed simulation model, and validation (PDF)

AUTHOR INFORMATION

Corresponding Author

*E-mail: km3b@andrew.cmu.edu.

ORCID ®

Francesca Lorandi: 0000-0001-5253-8468 Sajjad Dadashi-Silab: 0000-0002-4285-5846

Guojun Xie: 0000-0001-7020-1076 Xiangcheng Pan: 0000-0003-3344-4639

Krzysztof Matyjaszewski: 0000-0003-1960-3402

Notes

The authors declare no competing financial interest.

ACKNOWLEDGMENTS

Support from the National Science Foundation via grant DMR 1921858 is acknowledged.

REFERENCES

- (1) Chefary, J.; Chong, Y. K.; Ercole, F.; Krstina, J.; Jeffrey, J.; Le, T. P. T.; Mayadunne, R. T. A.; Meijs, G. F.; Moad, C. L.; Moad, G.; Rizzardo, E.; Thang, S. H. Living Free-Radical Polymerization by Reversible Addition-Fragmentation Chain Transfer: The RAFT Process. *Macromolecules* 1998, 31, 5559–5562.
- (2) Perrier, S. Anniversary Perspective: RAFT Polymerization A User Guide. *Macromolecules* **2017**, *50*, 7433–7447.
- (3) Hawker, C. J.; Bosman, A. W.; Harth, E. New polymer synthesis by nitroxide mediated living radical polymerizations. *Chem. Rev.* **2001**, *101*, 3661–3688.
- (4) Nicolas, J.; Guillaneuf, Y.; Lefay, C.; Bertin, D.; Gigmes, D.; Charleux, B. Nitroxide-mediated polymerization. *Prog. Polym. Sci.* **2013**, *38*, 63–235.
- (5) Tebben, L.; Studer, A. Nitroxides: Applications in Synthesis and in Polymer Chemistry. *Angew. Chem., Int. Ed.* **2011**, *50*, 5034–5068.
- (6) Wang, J.-S.; Matyjaszewski, K. Controlled Living Radical Polymerization Atom-Transfer Radical Polymerization in the Presence of Transition-Metal Complexes. *J. Am. Chem. Soc.* **1995**, 117, 5614–5615.
- (7) Matyjaszewski, K.; Xia, J. Atom transfer radical polymerization. *Chem. Rev.* **2001**, *101*, 2921–2990.
- (8) Kamigaito, M.; Ando, T.; Sawamoto, M. Metal-Catalyzed Living Radical Polymerization. *Chem. Rev.* **2001**, *101*, 3689–3746.
- (9) Matyjaszewski, K.; Tsarevsky, N. V. Macromolecular Engineering by Atom Transfer Radical Polymerization. *J. Am. Chem. Soc.* **2014**, 136, 6513–6533.
- (10) Matyjaszewski, K. Advanced Materials by Atom Transfer Radical Polymerization. *Adv. Mater.* **2018**, *30*, 1706441.
- (11) Matyjaszewski, K. Atom Transfer Radical Polymerization (ATRP): Current Status and Future Perspectives. *Macromolecules* **2012**, *45*, 4015–4039.
- (12) Tsarevsky, N. V.; Matyjaszewski, K. "Green" Atom Transfer Radical Polymerization: From Process Design to Preparation of Well-Defined Environmentally Friendly Polymeric Materials. *Chem. Rev.* **2007**, *107*, 2270–2299.
- (13) Matyjaszewski, K.; Jakubowski, W.; Min, K.; Tang, W.; Huang, J.; Braunecker, W. A.; Tsarevsky, N. V. Diminishing catalyst concentration in atom transfer radical polymerization with reducing agents. *Proc. Natl. Acad. Sci. U.S.A.* **2006**, *103*, 15309–15314.
- (14) Konkolewicz, D.; Magenau, A. J. D.; Averick, S. E.; Simakova, A.; He, H.; Matyjaszewski, K. ICAR ATRP with ppm Cu Catalyst in Water. *Macromolecules* **2012**, *45*, 4461–4468.
- (15) Min, K.; Gao, H.; Matyjaszewski, K. Preparation of homopolymers and block copolymers in miniemulsion by ATRP using activators generated by electron transfer (AGET). *J. Am. Chem. Soc.* **2005**, *127*, 3825–3830.
- (16) Jakubowski, W.; Matyjaszewski, K. Activators regenerated by electron transfer for atom-transfer radical polymerization of (meth)-acrylates and related block copolymers. *Angew. Chem., Int. Ed.* **2006**, 45, 4482–4486.
- (17) Konkolewicz, D.; Wang, Y.; Krys, P.; Zhong, M.; Isse, A. A.; Gennaro, A.; Matyjaszewski, K. SARA ATRP or SET-LRP. End of controversy? *Polym. Chem.* **2014**, *5*, 4409.

(18) Konkolewicz, D.; Wang, Y.; Zhong, M.; Krys, P.; Isse, A. A.; Gennaro, A.; Matyjaszewski, K. Reversible-Deactivation Radical Polymerization in the Presence of Metallic Copper. A Critical Assessment of the SARA ATRP and SET-LRP Mechanisms. *Macromolecules* **2013**, *46*, 8749–8772.

- (19) Matyjaszewski, K.; Coca, S.; Gaynor, S. G.; Wei, M.; Woodworth, B. E. Zerovalent metals in controlled "living" radical polymerization. *Macromolecules* **1997**, *30*, 7348–7350.
- (20) Anastasaki, A.; Nikolaou, V.; Nurumbetov, G.; Wilson, P.; Kempe, K.; Quinn, J. F.; Davis, T. P.; Whittaker, M. R.; Haddleton, D. M. Cu(0)-Mediated Living Radical Polymerization: A Versatile Tool for Materials Synthesis. *Chem. Rev.* **2016**, *116*, 835–877.
- (21) Boyer, C.; Corrigan, N. A.; Jung, K.; Nguyen, D.; Nguyen, T.-K.; Adnan, N. N. M.; Oliver, S.; Shanmugam, S.; Yeow, J. Copper-Mediated Living Radical Polymerization (Atom Transfer Radical Polymerization and Copper(0) Mediated Polymerization): From Fundamentals to Bioapplications. *Chem. Rev.* **2016**, *116*, 1803–1949.
- (22) Williams, V. A.; Ribelli, T. G.; Chmielarz, P.; Park, S.; Matyjaszewski, K. A silver bullet: elemental silver as an efficient reducing agent for atom transfer radical polymerization of acrylates. *J. Am. Chem. Soc.* **2015**, *137*, 1428–1431.
- (23) Magenau, A. J. D.; Strandwitz, N. C.; Gennaro, A.; Matyjaszewski, K. Electrochemically Mediated Atom Transfer Radical Polymerization. *Science* **2011**, 332, 81–84.
- (24) Li, B.; Yu, B.; Huck, W. T. S.; Zhou, F.; Liu, W. Electrochemically Induced Surface-Initiated Atom-Transfer Radical Polymerization. *Angew. Chem., Int. Ed.* **2012**, *51*, 5092–5095.
- (25) Li, B.; Yu, B.; Huck, W. T. S.; Liu, W.; Zhou, F. Electrochemically Mediated Atom Transfer Radical Polymerization on Nonconducting Substrates: Controlled Brush Growth through Catalyst Diffusion. *J. Am. Chem. Soc.* **2013**, *135*, 1708–1710.
- (26) Shida, N.; Koizumi, Y.; Nishiyama, H.; Tomita, I.; Inagi, S. Electrochemically Mediated Atom Transfer Radical Polymerization from a Substrate Surface Manipulated by Bipolar Electrolysis: Fabrication of Gradient and Patterned Polymer Brushes. *Angew. Chem., Int. Ed.* **2015**, *54*, 3922–3926.
- (27) Chmielarz, P.; Fantin, M.; Park, S.; Isse, A. A.; Gennaro, A.; Magenau, A. J. D.; Sobkowiak, A.; Matyjaszewski, K. Electrochemically mediated atom transfer radical polymerization (eATRP). *Prog. Polym. Sci.* **2017**, *69*, 47–78.
- (28) Tasdelen, M. A.; Uygun, M.; Yagci, Y. Photoinduced Controlled Radical Polymerization in Methanol. *Macromol. Chem. Phys.* **2010**, 211, 2271–2275.
- (29) Tasdelen, M. A.; Uygun, M.; Yagci, Y. Photoinduced Controlled Radical Polymerization. *Macromol. Rapid Commun.* **2011**, 32, 58–62.
- (30) Mosnáček, J.; Ilčíková, M. Photochemically Mediated Atom Transfer Radical Polymerization of Methyl Methacrylate Using ppm Amounts of Catalyst. *Macromolecules* **2012**, *45*, 5859–5865.
- (31) Konkolewicz, D.; Schröder, K.; Buback, J.; Bernhard, S.; Matyjaszewski, K. Visible Light and Sunlight Photoinduced ATRP with ppm of Cu Catalyst. ACS Macro Lett. 2012, 1, 1219–1223.
- (32) Anastasaki, A.; Nikolaou, V.; Zhang, Q.; Burns, J.; Samanta, S. R.; Waldron, C.; Haddleton, A. J.; McHale, R.; Fox, D.; Percec, V.; Wilson, P.; Haddleton, D. M. Copper(II)/Tertiary Amine Synergy in Photoinduced Living Radical Polymerization: Accelerated Synthesis of ω -Functional and α,ω -Heterofunctional Poly(acrylates). *J. Am. Chem. Soc.* **2014**, *136*, 1141–1149.
- (33) Ribelli, T. G.; Konkolewicz, D.; Bernhard, S.; Matyjaszewski, K. How are Radicals (Re)Generated in Photochemical ATRP? *J. Am. Chem. Soc.* **2014**, *136*, 13303–13312.
- (34) Dadashi-Silab, S.; Tasdelen, M. A.; Kiskan, B.; Wang, X.; Antonietti, M.; Yagci, Y. Photochemically Mediated Atom Transfer Radical Polymerization Using Polymeric Semiconductor Mesoporous Graphitic Carbon Nitride. *Macromol. Chem. Phys.* **2014**, *215*, 675–681
- (35) Fors, B. P.; Hawker, C. J. Control of a Living Radical Polymerization of Methacrylates by Light. *Angew. Chem., Int. Ed.* **2012**, *51*, 8850–8853.

(36) Discekici, E. H.; Anastasaki, A.; Kaminker, R.; Willenbacher, J.; Truong, N. P.; Fleischmann, C.; Oschmann, B.; Lunn, D. J.; Read de Alaniz, J.; Davis, T. P.; Bates, C. M.; Hawker, C. J. Light-Mediated Atom Transfer Radical Polymerization of Semi-Fluorinated (Meth)acrylates: Facile Access to Functional Materials. *J. Am. Chem. Soc.* 2017, 139, 5939–5945.

- (37) Pan, X.; Tasdelen, M. A.; Laun, J.; Junkers, T.; Yagci, Y.; Matyjaszewski, K. Photomediated controlled radical polymerization. *Prog. Polym. Sci.* **2016**, *62*, 73–125.
- (38) Mohapatra, H.; Kleiman, M.; Esser-Kahn, A. P. Mechanically controlled radical polymerization initiated by ultrasound. *Nat. Chem.* **2017**, *9*, 135–139.
- (39) Wang, Z.; Pan, X.; Yan, J.; Dadashi-Silab, S.; Xie, G.; Zhang, J.; Wang, Z.; Xia, H.; Matyjaszewski, K. Temporal Control in Mechanically Controlled Atom Transfer Radical Polymerization Using Low ppm of Cu Catalyst. ACS Macro Lett. 2017, 6, 546–549.
- (40) Dadashi-Silab, S.; Doran, S.; Yagci, Y. Photoinduced Electron Transfer Reactions for Macromolecular Syntheses. *Chem. Rev.* **2016**, *116*, 10212–10275.
- (41) Chen, M.; Zhong, M.; Johnson, J. A. Light-Controlled Radical Polymerization: Mechanisms, Methods, and Applications. *Chem. Rev.* **2016**, *116*, 10167–10211.
- (42) Corrigan, N.; Shanmugam, S.; Xu, J.; Boyer, C. Photocatalysis in organic and polymer synthesis. *Chem. Soc. Rev.* **2016**, *45*, 6165–6212.
- (43) Shanmugam, S.; Xu, J.; Boyer, C. Photocontrolled Living Polymerization Systems with Reversible Deactivations through Electron and Energy Transfer. *Macromol. Rapid Commun.* **2017**, *38*, 1700143.
- (44) Dadashi-Silab, S.; Atilla Tasdelen, M.; Yagci, Y. Photoinitiated Atom Transfer Radical Polymerization: Current Status and Future Perspectives. *J. Polym. Sci., Part A: Polym. Chem.* **2014**, *52*, 2878–2888.
- (45) Treat, N. J.; Sprafke, H.; Kramer, J. W.; Clark, P. G.; Barton, B. E.; Read de Alaniz, J.; Fors, B. P.; Hawker, C. J. Metal-Free Atom Transfer Radical Polymerization. *J. Am. Chem. Soc.* **2014**, *136*, 16096–16101.
- (46) Theriot, J. C.; McCarthy, B. G.; Lim, C.-H.; Miyake, G. M. Organocatalyzed Atom Transfer Radical Polymerization: Perspectives on Catalyst Design and Performance. *Macromol. Rapid Commun.* **2017**, 38, 1700040.
- (47) Pan, X.; Lamson, M.; Yan, J.; Matyjaszewski, K. Photoinduced Metal-Free Atom Transfer Radical Polymerization of Acrylonitrile. *ACS Macro Lett.* **2015**, *4*, 192–196.
- (48) Pan, X.; Fang, C.; Fantin, M.; Malhotra, N.; So, W. Y.; Peteanu, L. A.; Isse, A. A.; Gennaro, A.; Liu, P.; Matyjaszewski, K. Mechanism of Photoinduced Metal-Free Atom Transfer Radical Polymerization: Experimental and Computational Studies. *J. Am. Chem. Soc.* **2016**, 138, 2411–2425.
- (49) Theriot, J. C.; Lim, C.-H.; Yang, H.; Ryan, M. D.; Musgrave, C. B.; Miyake, G. M. Organocatalyzed atom transfer radical polymerization driven by visible light. *Science* **2016**, *352*, 1082–1086.
- (50) Dadashi-Silab, S.; Pan, X.; Matyjaszewski, K. Phenyl Benzo-[b]phenothiazine as a Visible Light Photoredox Catalyst for Metal-Free Atom Transfer Radical Polymerization. *Chem.—Eur. J.* **2017**, 23, 5972—5977.
- (51) Corrigan, N.; Xu, J.; Boyer, C.; Allonas, X. Exploration of the PET-RAFT Initiation Mechanism for Two Commonly Used Photocatalysts. *ChemPhotoChem* **2019**, *3*, 1193–1199.
- (52) Xu, J.; Shanmugam, S.; Fu, C.; Aguey-Zinsou, K.-F.; Boyer, C. Selective Photoactivation: From a Single Unit Monomer Insertion Reaction to Controlled Polymer Architectures. *J. Am. Chem. Soc.* **2016**, *138*, 3094–3106.
- (53) Shanmugam, S.; Xu, J.; Boyer, C. Exploiting Metalloporphyrins for Selective Living Radical Polymerization Tunable over Visible Wavelengths. *J. Am. Chem. Soc.* **2015**, *137*, 9174–9185.
- (54) Xu, J.; Jung, K.; Boyer, C. Oxygen Tolerance Study of Photoinduced Electron Transfer-Reversible Addition-Fragmenta-

tion Chain Transfer (PET-RAFT) Polymerization Mediated by Ru(bpy)3Cl2. *Macromolecules* **2014**, 47, 4217–4229.

- (55) Ribelli, T. G.; Augustine, K. F.; Fantin, M.; Krys, P.; Poli, R.; Matyjaszewski, K. Disproportionation or Combination? The Termination of Acrylate Radicals in ATRP. *Macromolecules* **2017**, *50*, 7920–7929.
- (56) Dadashi-Silab, S.; Matyjaszewski, K. Temporal Control in Atom Transfer Radical Polymerization Using Zerovalent Metals. *Macromolecules* **2018**, *51*, 4250–4258.
- (57) Wang, Y.; Soerensen, N.; Zhong, M.; Schroeder, H.; Buback, M.; Matyjaszewski, K. Improving the "Livingness" of ATRP by Reducing Cu Catalyst Concentration. *Macromolecules* **2013**, *46*, 683–691
- (58) Ribelli, T. G.; Wahidur Rahaman, S. M.; Daran, J.-C.; Krys, P.; Matyjaszewski, K.; Poli, R. Effect of Ligand Structure on the CuII–R OMRP Dormant Species and Its Consequences for Catalytic Radical Termination in ATRP. *Macromolecules* **2016**, *49*, 7749–7757.
- (59) Nakamura, Y.; Ogihara, T.; Yamago, S. Mechanism of Cu(I)/Cu(0)-Mediated Reductive Coupling Reactions of Bromine-Terminated Polyacrylates, Polymethacrylates, and Polystyrene. *ACS Macro Lett.* **2016**, *5*, 248–252.
- (60) Fantin, M.; Lorandi, F.; Ribelli, T. G.; Szczepaniak, G.; Enciso, A. E.; Fliedel, C.; Thevenin, L.; Isse, A. A.; Poli, R.; Matyjaszewski, K. Impact of Organometallic Intermediates on Copper-Catalyzed Atom Transfer Radical Polymerization. *Macromolecules* **2019**, *52*, 4079–4090.
- (61) Thevenin, L.; Fliedel, C.; Fantin, M.; Ribelli, T. G.; Matyjaszewski, K.; Poli, R. Reductive Termination of Cyanoisopropyl Radicals by Copper(I) Complexes and Proton Donors: Organometallic Intermediates or Coupled Proton-Electron Transfer? *Inorg. Chem.* **2019**, *58*, 6445–6457.
- (62) Thevenin, L.; Fliedel, C.; Matyjaszewski, K.; Poli, R. Impact of Catalyzed Radical Termination (CRT) and Reductive Radical Termination (RRT) in Metal-Mediated Radical Polymerization Processes. *Eur. J. Inorg. Chem.* **2019**, 2019, 4489–4499.
- (63) Xie, G.; Martinez, M. R.; Daniel, W. F. M.; Keith, A. N.; Ribelli, T. G.; Fantin, M.; Sheiko, S. S.; Matyjaszewski, K. The Benefits of Catalyzed Radical Termination: High-Yield Synthesis of Polyacrylate Molecular Bottlebrushes without Gelation. *Macromolecules* **2018**, *51*, 6218–6225.
- (64) Tang, W.; Matyjaszewski, K. Effect of Ligand Structure on Activation Rate Constants in ATRP. *Macromolecules* **2006**, 39, 4953–
- (65) Schröder, K.; Mathers, R. T.; Buback, J.; Konkolewicz, D.; Magenau, A. J. D.; Matyjaszewski, K. Substituted Tris(2-pyridylmethyl)amine Ligands for Highly Active ATRP Catalysts. ACS Macro Lett. 2012, 1, 1037–1040.
- (66) Whitfield, R.; Parkatzidis, K.; Rolland, M.; Truong, N. P.; Anastasaki, A. Tuning Dispersity by Photoinduced Atom Transfer Radical Polymerisation: Monomodal Distributions with ppm Copper Concentration. *Angew. Chem., Int. Ed.* **2019**, *58*, 13323–13328.
- (67) Jakubowski, W.; Min, K.; Matyjaszewski, K. Activators Regenerated by Electron Transfer for Atom Transfer Radical Polymerization of Styrene. *Macromolecules* **2006**, *39*, 39–45.
- (68) Wulkow, M. Computer Aided Modeling of Polymer Reaction Engineering-The Status of Predici, I-Simulation. *Macromol. React. Eng.* **2008**, 2, 461–494.
- (69) Tang, W.; Kwak, Y.; Braunecker, W.; Tsarevsky, N. V.; Coote, M. L.; Matyjaszewski, K. Understanding Atom Transfer Radical Polymerization: Effect of Ligand and Initiator Structures on the Equilibrium Constants. J. Am. Chem. Soc. 2008, 130, 10702–10713.
- (70) Krys, P.; Fantin, M.; Mendonça, P. V.; Abreu, C. M. R.; Guliashvili, T.; Rosa, J.; Santos, L. O.; Serra, A. C.; Matyjaszewski, K.; Coelho, J. F. J. Mechanism of supplemental activator and reducing agent atom transfer radical polymerization mediated by inorganic sulfites: experimental measurements and kinetic simulations. *Polym. Chem.* **2017**, *8*, 6506–6519.
- (71) Dervaux, B.; Junkers, T.; Schneider-Baumann, M.; Du Prez, F. E.; Barner-Kowollik, C. Propagation rate coefficients of isobornyl

acrylate, tert-butyl acrylate and 1-ethoxyethyl acrylate: A high frequency PLP-SEC study. *J. Polym. Sci., Part A: Polym. Chem.* **2009**, 47, 6641–6654.

- (72) Barth, J.; Buback, M.; Russell, G. T.; Smolne, S. Chain-Length-Dependent Termination in Radical Polymerization of Acrylates. *Macromol. Chem. Phys.* **2011**, 212, 1366–1378.
- (73) Tang, W.; Kwak, Y.; Braunecker, W.; Tsarevsky, N. V.; Coote, M. L.; Matyjaszewski, K. Understanding Atom Transfer Radical Polymerization: Effect of Ligand and Initiator Structures on the Equilibrium Constants. *J. Am. Chem. Soc.* **2008**, *130*, 10702–10713.
- (74) Lorandi, F.; Matyjaszewski, K. Why Do We Need More Active ATRP Catalysts? *Isr. J. Chem.* **2019**, DOI: 10.1002/ijch.201900079.
- (75) Doan, V.; Noble, B. B.; Fung, A. K. K.; Coote, M. L. Rational Design of Highly Activating Ligands for Cu-Based Atom Transfer Radical Polymerization. *J. Org. Chem.* **2019**, *84*, 15624–15632.
- (76) Paturej, J.; Sheiko, S. S.; Panyukov, S.; Rubinstein, M. Molecular structure of bottlebrush polymers in melts. *Sci. Adv.* **2016**, *2*, No. e1601478.
- (77) Sumerlin, B. S.; Neugebauer, D.; Matyjaszewski, K. Initiation Efficiency in the Synthesis of Molecular Brushes by Grafting from via Atom Transfer Radical Polymerization. *Macromolecules* **2005**, *38*, 702–708.